

Constraining $U(1)_{L_\mu-L_\tau}$ charged dark matter model for muon $g-2$ anomaly with AMS-02 electron and positron data

Lei Zu,^{1,2} Xu Pan,^{1,2} Lei Feng*,^{1,3} Qiang Yuan,^{1,2} and Yi-Zhong Fan^{†1,2}

¹Key Laboratory of Dark Matter and Space Astronomy,

Purple Mountain Observatory, Chinese Academy of Sciences, Nanjing 210023, China

²School of Astronomy and Space Science, University of Science and Technology of China, Hefei, Anhui 230026, China

³Joint Center for Particle, Nuclear Physics and Cosmology,

Nanjing University – Purple Mountain Observatory, Nanjing 210093, China

Very recently, the Fermi-Lab reported the new experimental combined results on the magnetic momentum of muon with a 4.2σ discrepancy compared with the expectation of the Standard Model [1]. A new light gauge boson X in the $L_\mu - L_\tau$ model provides a good explanation for the $g-2$ anomaly. A Dirac fermion dark matter with a large $L_\mu - L_\tau$ charge can explain both the $g-2$ anomaly and the dark matter relic density [2]. In this work, we focus on the case that the mass of the dark matter is larger than the mass of muon (i.e. $m_\Psi > m_\mu$) for which the channel $\Psi\Psi \rightarrow \mu^- \mu^+$ opens. Although the cross section $(\sigma v)_{\mu^- \mu^+}$ is smaller by a factor of $1/q_\Psi^2$ (q_Ψ represents the $L_\mu - L_\tau$ charge of the dark matter) compared with the channel $\Psi\Psi \rightarrow XX \rightarrow \nu\nu\bar{\nu}\bar{\nu}$, the resulting secondary electrons and positrons could imprint on their spectra above GeV energies due to the reacceleration effect of cosmic ray propagation. We use the AMS-02 measurements of electrons and positrons to constrain the annihilation cross section of the channel $\Psi\Psi \rightarrow \mu^- \mu^+$, which rules out part of the parameter space of the large $L_\mu - L_\tau$ charged dark matter model to account for the muon $g-2$ anomaly.

PACS numbers: 03.65.Nk

I. INTRODUCTION

Over the past decades, the Standard Model (SM) of particle physics achieved a great success. However, it still faces severe challenges when confronting some experimental anomalies, such as the dark matter (DM), the mass of neutrinos, and the muon $g-2$ anomaly [3–5]. Recently, the Fermi-lab reported a combined 4.2σ discrepancy of the muon $g-2$ measurement from the SM prediction [1]. Such a tension raises a big challenge to the SM. Many models containing new interactions with the muon sector were proposed to explain this tension [5–8]. The $U(1)_{L_\mu-L_\tau}$ model, which assumes a local gauge symmetry, provides naturally a gauge boson X to interact with the muon and can account for the $g-2$ anomaly [9–12]. This well-studied $L_\mu - L_\tau$ model with an MeV scale boson could also avoid the constraints from other experiments [13–15].

The $L_\mu - L_\tau$ model has also been widely studied to explain the relic density of DM, the mass of neutrinos, and the Galactic centre gamma ray excess [16–18]. However, usually a heavy mass of X is needed which was inconsistent with other experiments [13–15]. Recently, Ref. [2] proposed an SM singlet Dirac DM (Ψ) model with an $L_\mu - L_\tau$ charge q_Ψ . Distinct from the large mass of $O(10^3)$ GeV of X and DM required to explain the relic density in [16, 17], this additional q_Ψ parameter can explain the DM relic density with much lighter X and DM

particles. The cross section for $\Psi\Psi \rightarrow \mu^- \mu^+$ is smaller than $\Psi\Psi \rightarrow XX \rightarrow \nu\nu\bar{\nu}\bar{\nu}$ by a factor q_Ψ^2 for $m_\Psi > m_X$. The free parameter q_Ψ opens a new window to explain both the $g-2$ anomaly and the DM relic density, which is also consistent with other experiment limits. Following [2], we focus on the case $m_\Psi > m_\mu > m_X$, in which the channel $\Psi\Psi \rightarrow \mu^- \mu^+$ opens for the non-relativistic DM. Although the mass of DM can be small (e.g., $< \text{GeV}$), we argue that the secondary positrons and electrons from DM annihilation could also have a non-negligible effect on the GeV cosmic electron and positron spectrum due to the reacceleration effect, which can thus be probed by space-based detector like AMS-02. Parts of the parameter space to explain both the DM relic density and $g-2$ anomaly would be ruled out when considering the limits from AMS-02 data.

This work is organized as follows: In Section II, we introduce the $U(1)_{L_\mu-L_\tau}$ model that we used. In Section III we briefly describe the propagation and background of electrons and positrons. In Section IV, we set our constraints using the AMS-02 data. We conclude this work in Section V.

II. $L_\mu - L_\tau$ MODEL

In this work, we have considered an extension of the SM with a simple extra local $U(1)_{L_\mu-L_\tau}$ symmetry to the SM Lagrangian. Therefore, the Lagrangian remains invariant under the $SU(3)_c \times SU(2)_L \times U(1) \times U(1)_{L_\mu-L_\tau}$ gauge symmetry. The DM considered here contains an additional charge q_Ψ . The charge q_Ψ for muon (tau) is $+1(-1)$ [2]. Although this large charge q_Ψ seems unnatu-

*Corresponding author: fenglei@pmo.ac.cn

†Corresponding author: yzf@pmo.ac.cn

ral for the theory, it is allowed phenomenologically. The Lagrangian is:

$$\begin{aligned} \mathcal{L} = \mathcal{L}_{\text{SM}} &- g_X X_\lambda (\bar{\mu} \gamma^\lambda \mu - \bar{\tau} \gamma^\lambda \tau + \nu_{\mu L}^- \gamma^\lambda \nu_{\mu L} - \nu_{\tau L}^- \gamma^\lambda \nu_{\tau L}) \\ &- \frac{1}{4} X_{\mu\nu} X^{\mu\nu} + \frac{1}{2} m_X^2 X_\mu X^\mu \\ &+ \bar{\Psi} (i \not{\partial} - m_\Psi) \Psi - q_\Psi g_X X_\lambda \bar{\Psi} \gamma^\lambda \Psi, \end{aligned} \quad (1)$$

where X^μ and Ψ denotes the $U(1)_{L_\mu-L_\tau}$ gauge boson and Dirac DM, $X^{\mu\nu}$ is the field strength of X^μ . We have ignored the kinetic mixing and the right-hand neutrino terms since they are irrelevant for our phenomenological discussion below. Therefore we have four free parameters in this model: m_X , g_X , m_Ψ , q_Ψ .

The new combined result on the magnetic moment of muon measured by the Fermi-Lab shows a 4.2σ deviation from the SM

$$\Delta a_\mu = a_\mu^{\text{exp}} - a_\mu^{\text{SM}} = 251 \pm 59 \times 10^{-11} \quad (2)$$

The new gauge boson X could contribute to an extra magnetic moment of muon a_μ . The one-loop contribution is

$$\Delta a_\mu^X = \frac{g_X^2}{8\pi^2} \int_0^1 dx \frac{2m_\mu^2 x^2 (1-x)}{x^2 m_\mu^2 + (1-x)m_X^2}. \quad (3)$$

As discussed in [2, 5], with $g_X \sim 10^{-4}$ and $m_X \sim \text{O}(10)$ MeV, this gauge boson X could explain the $g-2$ anomaly and avoid the current experimental limits (see Fig. 1 in [2] and Fig. 32 in [5]).

In this work, we focus on the case of $m_\Psi > m_\mu > m_X$. Thus DM could annihilate through $\Psi\Psi \rightarrow XX$ process following with $X \rightarrow \nu\bar{\nu}$. The cross section is

$$(\sigma v)_{XX} = \frac{(q_\Psi g_X)^4 (m_\Psi^2 - m_X^2)^{3/2}}{4\pi m_\Psi (2m_\Psi^2 - m_X^2)^2}. \quad (4)$$

This cross section is related to the s-channel process $\Psi\Psi \rightarrow \mu\mu$ (for $m_X \ll m_\Psi$) as

$$(\sigma v)_{\mu-\mu^+} = \frac{1 + m_\mu^2/(2m_\Psi^2)}{q_\Psi^2} (1 - m_\mu^2/m_\Psi^2)^{1/2} \times (\sigma v)_{XX}. \quad (5)$$

Roughly $(\sigma v)_{\mu-\mu^+}$ is q_Ψ^{-2} smaller than $(\sigma v)_{XX}$. The additional parameter q_Ψ is helpful to explain the DM abundance and can avoid the constraints from the cosmic microwave background (CMB) observations, $(\sigma v)_{f\bar{f}}/(2m_\Psi) \leq 5.1 \times 10^{-27} \text{ cm}^3 \text{ s}^{-1} \text{ GeV}^{-1}$ [19, 20]¹. The typical cross section to explain the DM abundance is [21]

$$(\sigma v)/2 \simeq 3 \times 10^{-26} \text{ cm}^3 \text{ s}^{-1}. \quad (6)$$

Therefore q_Ψ needs to be large enough that the dominating channel $\Psi\Psi \rightarrow XX \rightarrow \nu\bar{\nu}$ could reach the value required to give the correct DM abundance and the $\Psi\Psi \rightarrow f\bar{f}$ channel is consistent with the CMB limits.

In the case $m_\Psi > m_\mu$, the non-relativistic Ψ would also annihilate into $\mu\bar{\mu}$ in the Milky Way and contribute to the spectrum of cosmic ray electrons and positrons. After reacceleration in the propagation, the sub-GeV e^+e^- could be accelerated to higher energies [22], which are detectable for the space-based experiments like AMS-02.

III. COSMIC RAY ELECTRONS AND POSITRONS

A. Propagation

Cosmic ray electrons and positrons propagate diffusively in the Galaxy. Numerical tools have been developed to calculate the propagation of cosmic rays, such as GALPROP [23] and DRAGON [24]. In this work we adopt the LikeDM code [25] to calculate the propagation process. This package employs a Green's function method based on numerical tables obtained with GALPROP for given distribution of the source. This method has been verified to be a good approximation to the GALPROP result, and is much more efficient. The propagation framework is assumed to be diffusion plus reacceleration, which was found to be well consistent with the secondary and primary nuclei measured by AMS-02 [26, 27]. The propagation parameters we used include the diffusion coefficient $D(E) = \beta D_0 (E/4 \text{ GeV})^\delta$ with $D_0 = 1 \times 10^{29} \text{ cm}^2 \text{ s}^{-1}$ and $\delta = 0.33$, the Alfvénic speed which characterizes the reacceleration effect $v_A = 26.3 \text{ km s}^{-1}$ [28]. Low-energy cosmic rays are affected by the solar modulation. We adopt the simple force-field approximation with the modulation potential to calculate this effect [29]. The modulation potential we adopt is 0.6 GV. For the DM density profile, we adopt the typical NFW distribution [30] with local density $\rho_0 = 0.3 \text{ GeV cm}^{-3}$ [31]. The injected e^+e^- spectrum from $\Psi\Psi \rightarrow \mu^-\mu^+$ is calculated using the PPC4 package [32].

Fig. 1 shows the $e^- + e^+$ spectrum after the propagation, for $m_\Psi = 0.2 \text{ GeV}$ and $(\sigma v)_{\mu-\mu^+} = 3 \times 10^{-26} \text{ cm}^3 \text{ s}^{-1}$. The AMS-02 measurements are also shown for comparison [33]. We can see that the reacceleration effect accelerate electrons and positrons to higher energies than m_Ψ .

B. Background

Since we focus on the spectral features which are distinct from the ‘‘smooth’’ background, it is reasonable to fit the majority of the observational spectra by the background [34, 35]. We adopt the background model in [36], which includes three components, the primary e^- , sec-

¹ Following [2, 19, 20], here we adopt the conservative limit on the cross section with charged final states.

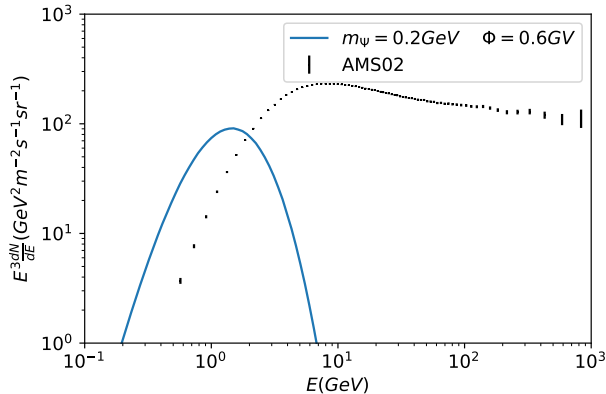


FIG. 1: Propagated $e^- + e^+$ spectrum from $\Psi\Psi \rightarrow \mu\bar{\mu}$ process, for $m_\Psi = 0.2$ GeV and $(\sigma v)_{\mu-\mu^+} = 3 \times 10^{-26}$ $\text{cm}^3 \text{s}^{-1}$. We assume a solar modulation potential of 0.6 GV.

ondary $e^- + e^+$, and an extra source term of $e^- + e^+$, i.e.,

$$\phi_{e^-} = C_{e^-} E^{-\gamma_1^{e^-}} [1 + (E/E_{br}^{e^-})^{\gamma_2^{e^-}}]^{-1} \exp(-E/E_c^{e^-}) \quad (7)$$

$$\phi_{e^+} = C_{e^+} E^{-\gamma_1^{e^+}} [1 + (E/E_{br}^{e^+})^{\gamma_2^{e^+}}]^{-1}, \quad (8)$$

$$\phi_s = C_s E^{-\gamma^s} \exp(-E/E_c^s). \quad (9)$$

The total background energy spectrum of $e^- + e^+$ is

$$\phi_{\text{bkg}, e^\pm} = \phi_{e^-} + 1.6\phi_{e^+} + 2\phi_s, \quad (10)$$

where the factor 1.6 is due to the asymmetry of the e^+ and e^- production in pp collisions [37]. The best-fit parameters we adopt can be found in Table. I of [36]. When we add the DM contribution in the model, we enable the backgrounds to vary to some degree by multiplying adjustment factors $\alpha_i E^{\beta_i}$, with $i=e^-, e^+, s$, on ϕ_{e^-} , ϕ_{e^+} , and ϕ_s , respectively, to optimize the fitting results [38].

IV. RESULTS

We use a maximum likelihood fitting to constrain the DM component. The data used include the AMS-02 positron fraction [39] and the total electron plus positron flux [33]. Assuming the DM annihilates to $\mu^- \mu^+$ in the Milky Way halo, we calculate the χ_0^2 (χ^2) without (with) the DM contribution. We set the 2σ upper limits on the DM annihilation cross section through setting $\Delta\chi^2 = \chi^2 - \chi_0^2 > 2.71$. The results are shown in Fig. 2. The limits on the $(\sigma v)_{\mu-\mu^+}$ change from 3×10^{-29} $\text{cm}^3 \text{s}^{-1}$ to 7×10^{-28} $\text{cm}^3 \text{s}^{-1}$, which are more stringent than the conservative CMB limits [2].

When we considering the $L_\mu - L_\tau$ model, we scan the parameters m_X and g_X for any given m_Ψ and q_Ψ to make sure these parameters are consistent with the current experimental limits. We calculate the $(\sigma v)_{XX}$ for each point to test whether the parameters can explain the DM abundance. The results are shown in Fig. 3.

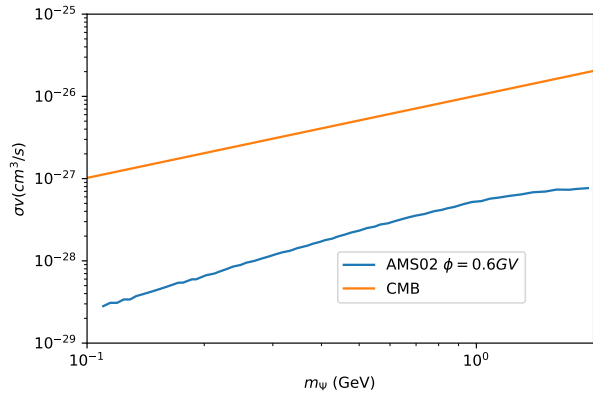


FIG. 2: The 2σ upper limits on the DM annihilation cross section $(\sigma v)_{\mu-\mu^+}$ through the process $\Psi\Psi \rightarrow \mu^- \mu^+$ as a function of DM mass (from 110 MeV to 2 GeV). The conservative CMB limits [2] are also shown in orange.

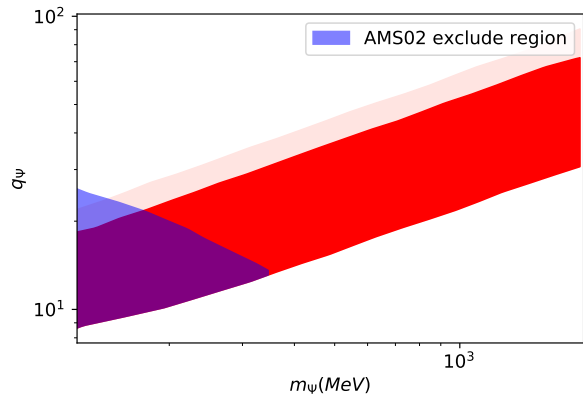


FIG. 3: The parameter space in the plane of m_Ψ and q_Ψ . The red (light red) region is favored by the $g-2$ at 1σ (2σ) confidence level together with the DM relic abundance. The shaded blue region is ruled out by the AMS-02 electron and positron spectra.

We find that the parameters with $110 \text{ MeV} < m_\Psi < 400 \text{ MeV}$ that can explain simultaneously the $g-2$ anomaly and the DM abundance are partly excluded by the AMS-02 data. The limits from AMS-02 are more stringent in the low mass range. For the $g-2$ anomaly and DM abundance favored regions (red regions), q_Ψ is smaller for lighter DM, and thus the q_Ψ^{-2} suppression factor of $(\sigma v)_{\mu-\mu^+}$ to $(\sigma v)_{XX}$ is bigger. For the same value $(\sigma v)_{XX}$ to explain the relic density, $(\sigma v)_{\mu-\mu^+}$ is larger, and hence the AMS-02 constraint is more stringent.

V. CONCLUSION

The $U(1)_{L_\mu - L_\tau}$ with an MeV scale gauge boson X could explain the $g-2$ anomaly well and avoid the lim-

its from other experiments. A large charged DM that is heavier than the muon and X particle could explain the DM abundance and also escape the constraints from the CMB. In this work, we use the AMS-02 electron and positron data to constrain this model. By means of the reacceleration effect of electrons and positrons in the Milky Way, low-energy electrons and positrons can be accelerated to the AMS-02 energy range, and can thus be strongly constrained. The limits for $(\sigma v)_{\mu-\mu^+}$ could

be down to $\sim 10^{-29} \text{ cm}^3 \text{ s}^{-1}$. Part of the parameter region to account for the $g-2$ anomaly can be excluded.

Acknowledgments This work is supported by the National Key Research and Development Program of China (Grant No. 2016YFA0400200), the National Natural Science Foundation of China (Grants No. U1738210, No. U1738136, and No. U1738206), Chinese Academy of Sciences, and the Program for Innovative Talents and Entrepreneur in Jiangsu.

-
- [1] B.Abi et.al.(Muon $g-2$ Collaboration) Measurement of the positive Muon Anomalous Magnetic Moment to 0.46 ppm. *Phys.Rev.Lett* **126**, 141801 (2021)
- [2] Kento Asai, Shohei Okawa and Koji Tsumura, Search for $U(1)_{L_\mu-L_\tau}$ charged Dark Matter with neutrino telescope, *JHEP*, **03**, 047 (2021)
- [3] E. Ma, M. Raidal, Neutrino mass, muon anomalous magnetic moment, and lepton flavor nonconservation, *Phys. Rev. Lett.* **87**, 011802 (2001)
- [4] E. Ma, Verifiable radiative seesaw mechanism of neutrino mass and dark matter, *Phys. Rev. D* **73**, 077301 (2006)
- [5] M. Lindner, M. Platscher and F. S. Queiroz, A Call for New Physics : The Muon Anomalous Magnetic Moment and Lepton Flavor Violation, *Phys. Rept.* **731**, 1–82 (2018)
- [6] G.-C. Cho, K. Hagiwara, Y. Matsumoto, D. Nomura, The MSSM confronts the precision electroweak data and the muon $g-2$, *JHEP* **11**, 068 (2011)
- [7] J. P. Miller, E. de Rafael, B. L. Roberts, D. Stckinger, Muon ($g-2$): Experiment and Theory, *Ann. Rev. Nucl. Part. Sci.* **62**, 237–264 (2012)
- [8] D. Stckinger, The muon magnetic moment and new physics, *Hyperfine Interact.* **214 (1-3)**, 13–19 (2013)
- [9] R. Foot, New Physics From Electric Charge Quantization?, *Mod. Phys. Lett. A* **6**, 527–530 (1991)
- [10] X. He, G. C. Joshi, H. Lew, and R. Volkas, NEW Z-prime PHENOMENOLOGY, *Phys. Rev. D* **43**, 22–24 (1991)
- [11] J. Heeck, W. Rodejohann, Gauged $L_\mu - L_\tau$ Symmetry at the Electroweak Scale, *Phys. Rev. D* **84**, 075007 (2011)
- [12] X.-J. Bi, X.-G. He, Q. Yuan, Parameters in a class of leptophilic models from PAMELA, ATIC and FERMI, *Phys. Lett. B* **678**, 168–173 (2009)
- [13] BaBar Collaboration, J. Lees et al., Search for a muonic dark force at BABAR, *Phys.Rev. D* **94**, no. 1 011102 (2016)
- [14] CCFR Collaboration, S. Mishra et al., Neutrino tridents and W Z interference, *Phys. Rev. Lett.* **66**, 3117–3120 (1991)
- [15] Y. Kaneta and T. Shimomura, On the possibility of a search for the $L_\mu - L_\tau$ gauge boson at Belle-II and neutrino beam experiments, *PTEP* 2017, no. 5 053B04. (2017)
- [16] Anirban Biswas, Sandhya Choubey and Sarif Khan, Neutrino Mass, Dark Matter and Anomalous Magnetic Moment of Muon in a $U(1)_{L_\mu-L_\tau}$ Model, *JHEP* **1609**, 147 (2016)
- [17] Sudhanwa Patra, Soumya Rao, Nirakar Sahoo, and Narendra Sahu, Gauged $U(1)_{L_\mu-L_\tau}$ model in light of muon $g-2$ anomaly, neutrino mass and dark matter phenomenology *Nuclear Phys B*, **917**, (317-336) (2017)
- [18] Zhi-Long Han, Ran Ding, Su-Jie Lin and Bin Zhu, Gauged $U(1)_{L_\mu-L_\tau}$ Scotogenic Model in light of R_{K^*} Anomaly and AMS-02 Positron Excess, *EPJC*, **79** 12.1007 (2019)
- [19] T. R. Slatyer, Indirect dark matter signatures in the cosmic dark ages. I. Generalizing the bound on s-wave dark matter annihilation from Planck results, *Phys. Rev. D* **93**, no. 2 023527 (2016)
- [20] R. K. Leane, T. R. Slatyer, J. F. Beacom, and K. C. Ng, GeV-scale thermal WIMPs: Not even slightly ruled out, *Phys. Rev. D* **98**, no. 2 023016 (2018)
- [21] K. Saikawa and S. Shirai, Precise WIMP Dark Matter Abundance and Standard Model Thermodynamics, *JCAP*, **08**, 011 (2020)
- [22] Mathieu Boudaud, Julien Lavalle and Pierre Salati, Novel Cosmic-Ray Electron and Positron Constraints on MeV Dark Matter Particles, *Phys. Rev. Lett.* **119**, 021103 (2017)
- [23] A. W. Strong and I. V. Moskalenko, Propagation of cosmic-ray nucleons in the Galaxy, *Astrophys. J.* **509**, 212 (1998)
- [24] C. Evoli, D. Gaggero, D. Grasso and L. Maccione, Cosmic-Ray Nuclei, Antiprotons and Gamma-rays in the Galaxy: a New Diffusion Model, *JCAP*, **10**, 018 (2008)
- [25] X. Huang, Y.-L. S. Tsai, and Q. Yuan, LikeDM: likelihood calculator of dark matter detection, *Comput. Phys. Commun.* **213**, 252 (2017)
- [26] Q. Yuan, S.-J. Lin, K. Fang, and X.-J. Bi, Propagation of cosmic rays in the AMS-02 era, *Phys. Rev. D* **95**, 083007 (2017)
- [27] Q. Yuan, C.-R. Zhu, X.-J. Bi, and D.-M. Wei. Secondary cosmic-ray nucleus spectra disfavor particle transport in the Galaxy without reacceleration, *J. Cosmol. Astropart. Phys.* **11**, 027 (2020)
- [28] M. Ackermann et al. LAT Collaboration, Fermi-LAT observations of the diffuse gamma-ray emission: implications for cosmic rays and the interstellar medium *Astrophys. J.* **750**, 3 (2012)
- [29] L. J. Gleeson and W. I. Axford, *Astrophys. J.* **154**, 1011 (1968)
- [30] J. F. Navarro, C. S. Frenk and S. D. M. White, A universal density profile from hierarchical clustering, *Astrophys. J.* **490**, 493 (1997)
- [31] G. Bertone, M. Cirelli, A. Strumia and M. Taoso, Gamma-ray and radio tests of the e^+e^- excess from DM annihilations, *JCAP* **0903**, 009 (2009)
- [32] M. Cirelli, G. Corcella, A. Hektor, G. Hutsi, M. Kadastik, P. Panci, M. Raidal, F. Sala, and A. Strumia, PPPC 4 DM ID: a poor particle physicist cookbook for dark matter indirect detection, *JCAP*, **03**, 051 (2011)

- [33] M. Aguilar et al., Precision Measurement of the $e^+ + e^-$ Flux in Primary Cosmic Rays from 0.5 GeV to 1 TeV with the Alpha Magnetic Spectrometer on the International Space Station, *Phys. Rev. Lett.* **113**, 221102 (2014)
- [34] L. Bergstrom, et al., New limits on dark matter annihilation from alpha magnetic spectrometer cosmic ray positron data, *Phys. Rev. Lett.*, **111**, 171101 (2013)
- [35] A. Ibarra, A. S. Lamperstorfer, J. Silk, Dark matter annihilations and decays after the AMS-02 positron measurements, *Phys. Rev. D*, **89**, 063539 (2014)
- [36] Lei Zu, Cun Zhang, Lei Feng, Qiang Yuan and Yi-Zhong Fan, Constraints on box-shaped cosmic ray electron feature from dark matter annihilation with the AMS-02 and DAMPE data, *Phys Rev D*.**98**, 063010 (2018)
- [37] T. Kamae, et al., Parameterization of γ , epm, and Neutrino Spectra Produced by pp Interaction in Astronomical Environments, *Astrophys. J.*, **647**, 692 (2006)
- [38] M. Cirelli, M. Kadastik, M. Raidal, and A. Strumia, Model-independent implications of the e, p cosmic ray spectra on properties of Dark Matter, *Nucl. Phys. B* **813**, 1 (2009)
- [39] M. Aguilar et al., First Result from the Alpha Magnetic Spectrometer on the International Space Station: Precision Measurement of the Positron Fraction in Primary Cosmic Rays of 0.5–350 GeV, *Phys. Rev. Lett.* **110**, 141102 (2013)